

Strain, Tensile and Hardness Laboratory Report

Dhruva Teja Turaga
02385740

Abstract

This report aims to use explain the background behind the Wheatstone bridge and how it can be used to get accurate readings of stress strain on metallic alloys. Additionally, the use of Tabor's construction to determine how accurate it is in getting the hardness of a material along with tensile tests on those materials to graph their true stress and strain. Using all these values we can evaluate their purposes in aerospace systems such as aluminium's primary advantage in strength, critical stress, and Young's modulus.

21/11/23



Contents

List of Figures	2
List of Tables	2
List of Symbols	3
1. Introduction	4
2. Theory and Background	4
Strain Measurement	4
Hardness Testing.....	5
3. Methodology.....	6
Strain Measurement	6
Hardness Testing.....	7
Tensile Testing.....	7
4. Results and Discussions.....	8
4.1. Graphs	8
4.2. Tables	11
4.3. Equations.....	12
5. Conclusions	13
Appendix.....	13

List of Figures

Figure 5. Amplified Voltage vs. Force	8
Figure 6. Stress vs. Strain for Copper, Brass & Aluminium.....	8
Figure 7. True Stress vs. True Strain for CFRP, Aluminium & Plastic.....	9
Figure 8. Stress vs. Strain for Aluminium including Tabor's Contraction.....	10
Figure 9. Stress vs. Strain for CFRP	10
Figure 10. Stress vs. Strain for Plastic	11
Figure 11. Hardness indentation photographs on Aluminium	11

List of Tables

Table 1 CFRP, Aluminium & Plastic statistics.....	11
Table 2 Hardness indentation statistics.....	12

List of Symbols

F	Force
L	Length
A	Cross Sectional area
E	Young's modulus
S	Gauge Factor
ρ	Resistivity
R	Resistance
H	Hardness
HV	Vickers Hardness
ΔR	Change in Resistance
V	Voltage
$GAIN$	Voltage Amplifier
ε_N	Nominal Strain
σ_N	Nominal Stress
ε_T	True Strain
σ_T	True Stress
σ_Y	Yield Stress
ε_o	Initial Strain
L_o	Initial gauge length
Hz	Hertz

1. Introduction

This experiment is aimed to test and quantify a material's resistance to different loads, specifically how much different materials can withstand under stress, as well as hardness for metallic alloys. There are going to be three different tests being conducted. Firstly, the strain measurement test which tests three different metallic alloys (Copper, Brass & Aluminium) along with a strain gauge to identify the extension it produces with different levels of stress. Secondly, the hardness test which occurs on the dog bone specimen of aluminium and is used to get photographs of the indent created by the hardness machine and calculate Vickers hardness to evaluate the quantity of micro-hardness. Finally, the tension test which stretches three materials (CFRP, aluminium & plastic), who are in a dog bone structure, until the material breaks (failure) to see how strain varies with different stresses applied on the materials.

2. Theory and Background

Strain Measurement

Minute changes in strain are very difficult to measure as the extensions are too small for either machines using springs or humans using rulers to calculate as the precision is very low. However, resistance strain gauges were developed to measure these small changes using the phenomenon by Lord Kelvin that electrical conductor resistances vary if they are deformed(1). The strain gauge is a serpentine conducting element securely bonded to a surface in which the strain produced on the surface in a specific direction is proportional to the strain in the conductor in the same direction. The reason behind this unique shape is that it maximises the length of the conductor which gets the maximum possible strain. Although, from this concept, many resistance strain gauges are produced the most used gauge is the wire strain due to its low cost and establishment as a product.

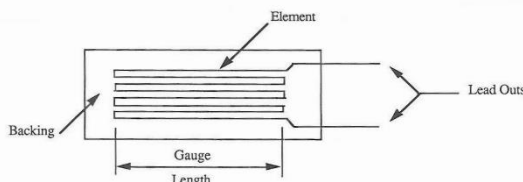


Figure 1: Anatomy of the strain gauge (2)

Since the strain gauge has a constant length, cross sectional area and resistivity we can calculate its resistance using equation 1. From this we can deduce that if strain isn't too large then the relative ΔR is proportional to the imposed strain which leads us to equation 2. The value S is a constant named the Gauge Factor which varies with based on materials & geometry of gauge, however, for many uses it is equal to 2.1. An issue arises with this method in which ΔR /electric flow is very hard to measure using a battery and traditional equipment as its magnitude is very small. This is where a Wheatstone Bridge is used.

A Wheatstone Bridge is a mechanism by which small changes in resistance can be measured with resistors in parallel to each other. By using Kirchhoff's Laws and basic definitions of circuits the voltage output can be calculated. Using the fact that all the resistors (initially) are all the same value, the bridge is balanced and ΔR is 0, if one of the resistors changes to the

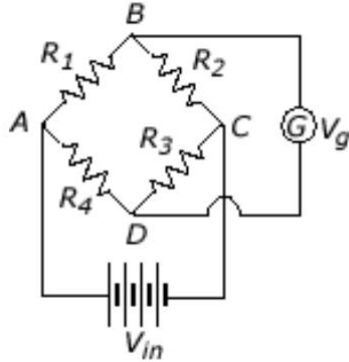


Figure 2: Schematic of the Wheatstone bridge (3)

strain gauge then the change in resistance is identifiable. For example, if we connect the strain gauge instead of R_1 , once deformed ΔR will not equal 0 and will give us equation 3. Combined with equation 2 we can manipulate to get equation 4. To make the value of V_g more useable, a voltage amplifier is used in addition to the

circuit which multiplies the output voltage by a constant factor called *GAIN* which we need to consider when calculating strain. This forms equation 5 which rearranged and substituted into our main equation gives us equation 6, which we can use to calculate the strain.

Another main advantage of the Wheatstone bridge is that by using a dummy strain gauge on the same material but unloaded. We can remove fictitious strain induced by thermal changes in the material by connecting the dummy gauge in series (R_2), this thermal compensation gives us an almost exact value for strain.

Hardness Testing

Hardness is defined as the resistance to penetration of a rigid, non-deformable object which can easily be quantified experimentally with the use of a rigid indenter. The amount of force applied by the indenter to the sample determines the extent of permanent indentation the terms hardness, micro-hardness, nano-hardness refer to indentations leaving footprints at mm, μm and nm length scales, respectively.

Using the classical definition of hardness, equation 6 can be created, A is the area of contact between indenter and material projected on the plane perpendicular to the applied load. The stress distribution, however, is important to look over. When indentation occurs on a dense & ductile material the formation of an approximately hemispherical region is made. This stress state is purely hydrostatic (compressive stresses is roughly equal to that of an inviscid fluid in equilibrium) and the diameter of this is approximately equal to the projected contact area. The region induces a roughly hemispherical finite outer shell of plasticity to form in which the material has yielded because of the indenter but not in hydrostatic conditions. Outside of this region, strains on the material are negligible and is therefore called the elastic regime and the material behaves normally.

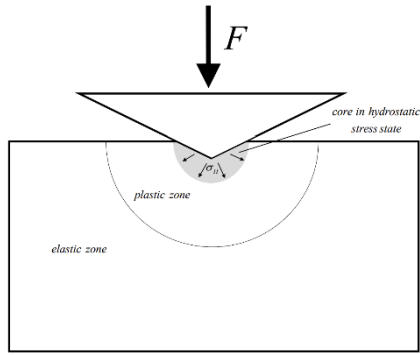


Figure 3: Elasto-plastic indentation of a solid by a sharp indenter (4)

When applying progressive indentation on a material whether by a nanometre or kilometre, the footprint remains the same which is defined as the self-similarity between indents. This then results in the hardness being independent of the indentation depth or force, the most common being Vickers. The reason for this being that the shape of the problem is self-similar at every length scale so then the strain field is also self-similar. As hardness is a mechanical property which depends more on yield stress than stiffness (E) since it is plastically governed. The relation between hardness and the inelastic response was first developed by Tabor (1951), who stated that the hardness(H) equals three times the flow stress at plastic strain in the range of 8-10% in most metals (5). This is usually taken by the standard deviation of the materials.

The Vickers indenter is a self-similar indenter with the shape of a square pyramid with opposite sides forming an angle of 136° . Vickers hardness (H_V) is historically defined in a different way than classical hardness as it takes the area of the lateral surface rather than projected surface (base of pyramid) and therefore we can define it using equation 8. This is measured in kgf/mm^2 with the form xxxHVyy/zz where xxx is the hardness, yy is the load and zz is the length of time which it is indented. This value, however, can change as the metal responds differently based on the length of exposure which can create pile-up and sink-in, this varies distance which is why the average needs to be taken and the distance between indents must be greater than 2mm.

3. Methodology

Strain Measurement

Initially we had to measure the cross-sectional areas(A) of the specimens using the vernier callipers at the gauge portion as well as gauge factor(S) used and GAIN amplifier ($GAIN$) which were given. Then we had to fasten the ends of the specimen to the ends of the hand-operated tensile machine carefully as to not induce initial stress to the piece. Then we connected the strain gauge wires to the turned off Wheatstone bridge. This was initially unbalanced, so we used the dial to balance the bridge until it was approximately zero. Once the bridge is turned on, we varied the load and measure the corresponding voltage after the amplifier is used. This was measured in 0.5 kN intervals from 0 to 3.5 loaded and unloaded. These values were noted down and the specimen is slowly and carefully removed and then replaced two more times with the other specimens. These values are then put into the formula to calculate the strain. We had to manipulate the data a lot but using equation 6 we could calculate the nominal strain and plot corresponding graphs of amplified voltage vs force and stress vs strain).

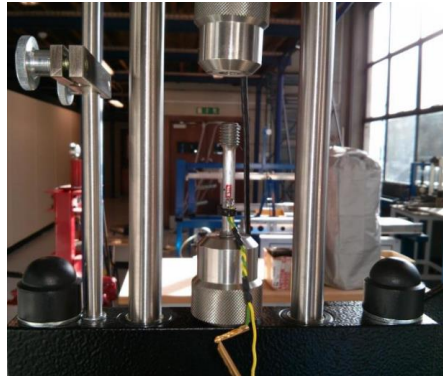


Figure 4: How specimen is used and loaded onto the extensometer (6)

Hardness Testing

The dog bone specimen of aluminium was sanded down with course and fine sandpaper until the surface was smooth which is then washed to remove any irregular pieces on the surface. The specimen was then placed into the test area of the microscope in which the correct region was identified, and indenter was used after it had been focussed by the fine focus knob. We were careful at this step as to not touch the table as it could cause imperfections within the indent. After which we used the eye piece to identify the corners of the indents and measured them vertically and horizontally. This then prompted the machine to give us the hardness value which we noted down. After this part of the specimen was used, we moved to another location roughly two or more millimetres away using the other knobs from the original indent, so we were safe from the plastic region then repeated it again four more times. We used these values to calculate the data in table 2.

Tensile Testing

For the tension test we conducted after the hardness test we used safety goggles and a plastic screen to prevent shards of the material eject and injure us. Initially we measured the width and depth of the cross section so we can determine the cross-sectional area using vernier callipers, we did this in three different locations so that an average which may have been formed by the manufacturing. Then we connected the first dog bone material to the machine jaw without inducing any load carefully. After which we balanced the reading of the load and displacement on the data acquisition software as initially with zero stress there should be zero strain after we put the displacement calculator at the right position. Then we used the wheel to slowly increase the load on the dog bone, approximately one per second as the rate at which data was taken was 1 Hz, then the displacement was taken on the graph. For specific specimens we unloaded the material and loaded again to see the response, but we continued with the same material until it failed in which case we stopped the data logger, carefully removed the specimen, and repeated. After each dog bone we saved the file in the correct location and continued. Since the values are noted with time, we had to arrange the values in time order and calculate the relative values (which are ε_N , σ_N , ε_T , σ_T and plotted them against each other and together to determine different values as stated in table 1).

4. Results and Discussions

4.1. Graphs

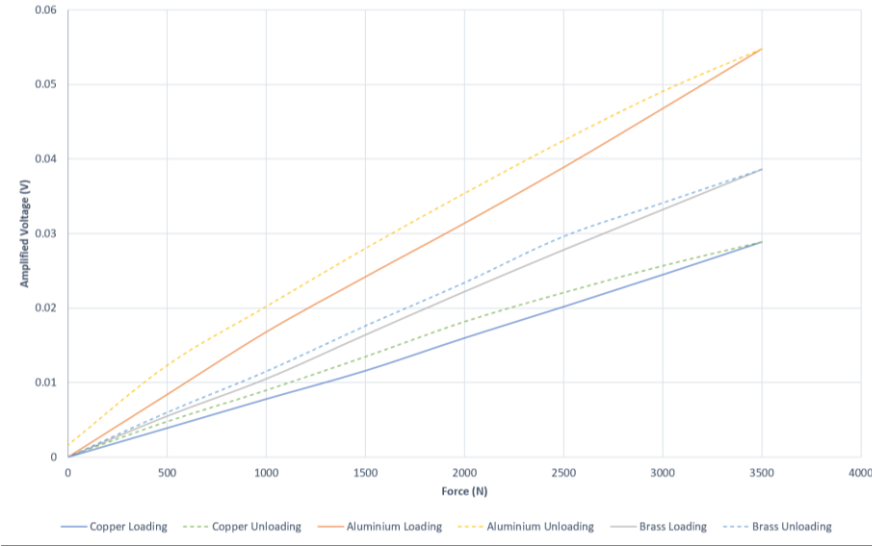


Figure 5. Amplified Voltage vs. Force

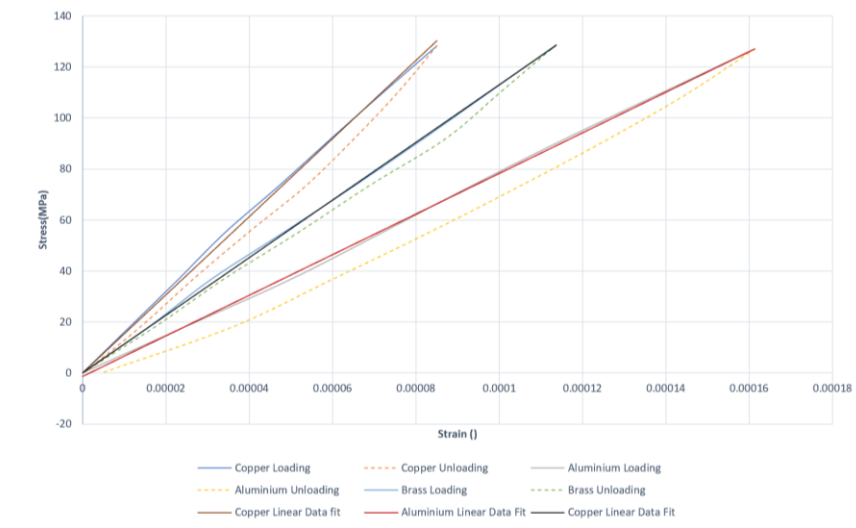


Figure 6. Stress vs. Strain for Copper, Brass & Aluminium

The graph in figure 4 shows that amplified voltage increases proportionally with the force applied across the metal alloys. From this we can predict that figure 5 also follows this trend as it relates to equation 6, we used for strain and with 4, V_{in} , S & $GAIN$ being constant. Therefore, strain is directly proportional to the voltage and so is stress to the force as we assumed the cross-sectional area remains constant. This prove our results are correct as the figures are similar, but the unloading didn't return to the original position, which means the material underwent plastic deformation once the stress was reduced. This tells us that energy was lost to the deformation of the material and therefore the discrepancy of this and true elastic materials highlights to us that there is no perfect elastic response to metals, but the proof of unloading tells us that these metals are ductile. The data within the figures 5 & 6 roughly lie on the trend line which shows how there were little anomalies however our data magnitude was quite small ($\times 10^{-3}$). This is specific for strain as most of the values were constants, but

stress was on an analogue scale which could have given rise to a parallax error more so than systematic.

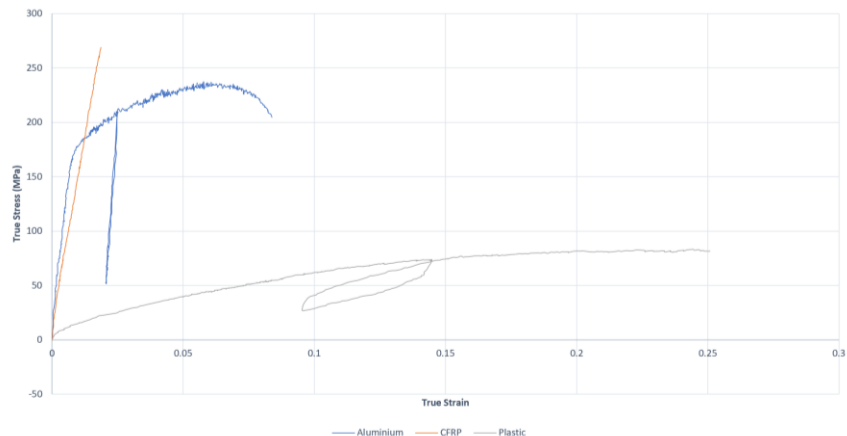


Figure 7. True Stress vs. True Strain for CFRP, Aluminium & Plastic

Figure 6 shows us the response of different materials to varying levels of stress and their relative strain. This graph considers the true stress against true strain which considers the constantly changing cross sectional area when stress and relative strain is measured making it a very accurate and realistic depiction of the material. Initially, CFRP has a very low ductility due to its sudden drop in strain as soon as a specific stress was applied, as well as this at its ultimate tensile point (which is much higher than the other materials) doesn't expand further into the plastic region of the material. This is different from aluminium and plastic who experience a significantly larger amount of plastic deformation, this is primarily due to the weak Van der Waals forces between the layers of carbon making it require less energy to completely break apart. The materials of plastic and aluminium underwent enough plastic deformation for them to be unloaded and figure 6 gives a very good image of how energy is lost in the unloading and reloading of the stress. Aluminium's unloading and reloading is very similar showing how very minimal energy is lost in the deformation, so the material doesn't heat up as much due to strong metallic bonds being difficult to move apart but plastic has high amounts of energy lost (forming the loop) as covalent bonds are breaking releasing lots of energy. This experiment could have a systematic error in which we measured the cross-sectional area incorrectly due to random errors like a not perfectly calibrated callipers as well as the force also being on an analogue meter again which creates parallax, despite this we took readings from one person with other people re-checking in the same position to guarantee the correct eye level reading.

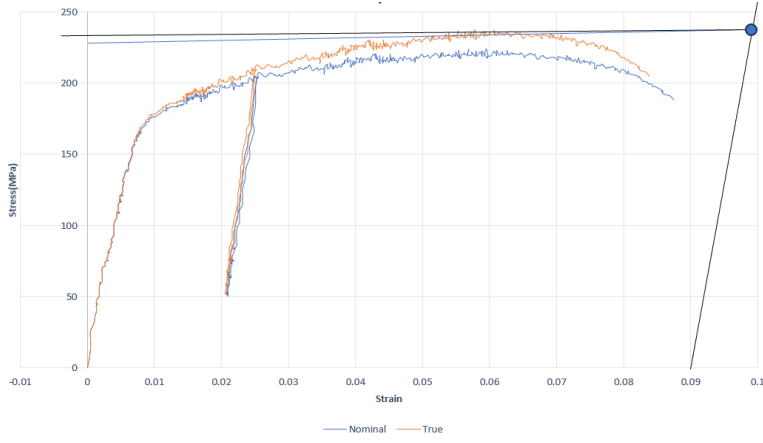


Figure 8. Stress vs. Strain for Aluminium including Tabor's Construction (True & Nominal)

Figure 7 depicts how the stress and strain values vary with the graph of true stress against true strain and nominal stress and strain. Based on the similarity of the graphs up to the yield point (σ_Y), this means the cross-sectional area changes negligibly the elastic part of the graph, this coincides with our theory as metals are very ductile and require a large amount of initial energy to break apart the metallic bonds. However, after this point they begin to separate as the cross-sectional area rapidly starts to decrease (unloading and reloading up to the ultimate tensile strength) after which it breaks. Looking at Tabor's construction, it reveals that the hardness achieved is not very far from the yield point and specifically it is within one standard deviation of the result which shows its accuracy and proof of concept.

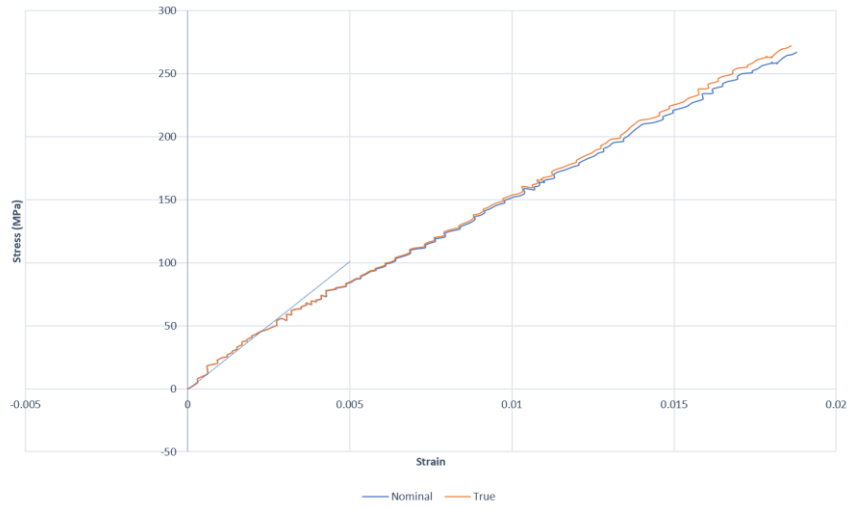


Figure 9. Stress vs. Strain for CFRP (True & Nominal)

Figure 8. Stress vs. Strain for CFRP which initially follows the same trend as the aluminium where the true and nominal are approximately equal as the area has little change. After this it starts to separate but much less than with the aluminium, this is since strain on this material doesn't increase the cross-sectional area enough, once the molecules in this composite are broken, all the forces are rapidly overcome to break it. This means that the cross section does not have sufficient time to change primarily due to the weak Van der Waal forces making this a very brittle material.

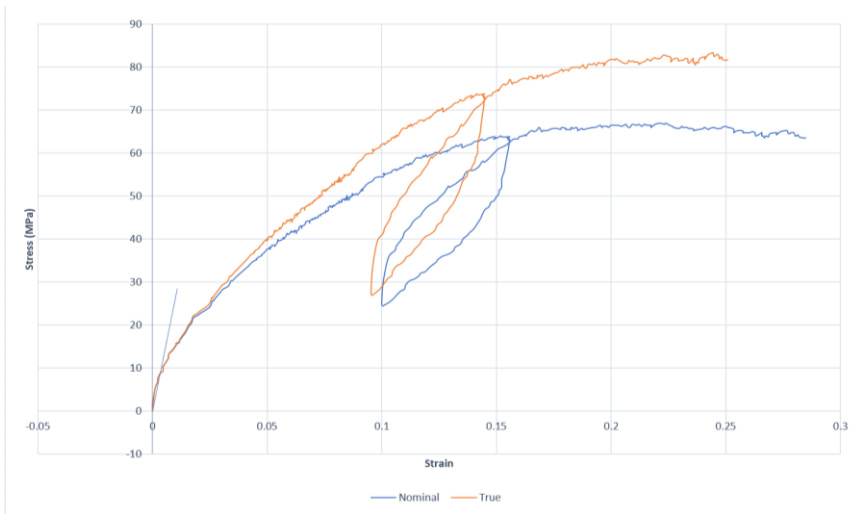


Figure 10. Stress vs. Strain for Plastic (True & Nominal)

Figure 8. Stress vs. Strain for plastic, this graph also follows the trend of the other two materials in which the true and nominal stress/strain curves are identical however, as soon as it passes the yield point, they very quickly become much more different. After the point at which plastic deformation starts the cross-sectional area differs massively as plastic is a very ductile like aluminium but the forces between the molecules are much easier to overcome but still have enough force, unlike CFRP, to keep shape. For this reason, the cross-sectional area decreases at a faster rate. Looking at the unloading and re-loading curve we can see that lots of energy is lost showing how after breaking the forces, lots of excess energy gets dissipated as heat within the material which makes the forces even weaker requiring less energy afterwards to break. This shows how the ultimate tensile strength of plastic is much less than that of aluminium.

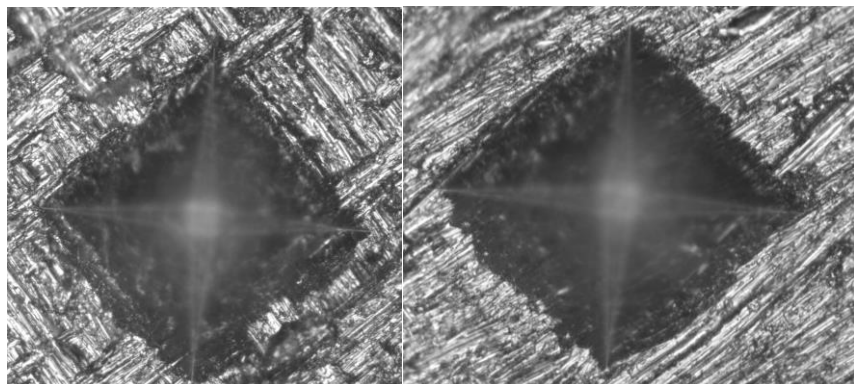


Figure 11. Hardness indentation photographs on Aluminium

Figure 10 shows us Vickers hardness indents on aluminium. These photographs were taken at ample distance from each other as to not be within plastic deformation hemisphere. These photographs however include higher uncertainties because the machine used has two lines which we needed to line up with the corners. This is very subjective but mitigated by multiple different people assessing the image before saving the file.

4.2. Tables

Table 1 CFRP, Aluminium & Plastic statistics

	Initial Cross-Sectional Area (m ²)	Initial Length (m)	Elastic Modulus (GPa)	Critical Stress (MPa)	UTS(MPa)	Ductility (%)	Specific Stiffness (MPa)	Specific Strength (KPa)
--	--	--------------------	-----------------------	-----------------------	----------	---------------	--------------------------	-------------------------

Aluminium	6.09628E-06	0.056	80	54	225	48.72	29.63	20
CFRP	5.46422E-06	0.08	40	166.67	166.67	23.28	14.81	61.73
Plastic	2.45217E-05	0.021	2.4	16	80	33.51	0.89	5.93

Table 1 shows us the different values we can interpret and calculate from the graphs. From the table we can see that the values estimated/assessed in each figure correctly matches with the values we have calculated. For many different applications this table can be useful for identifying the correct material. Comparing the specimens shows us that the material most stiff is aluminium along with it also being the most ductile and being able to withstand the most stress. However, although CFRP lacks the qualities of aluminium, its specific strength is much higher than that of the other two materials making it good for applications where weight is a very important factor. Plastic, on the other hand, which does not have all the advantages of the other two materials it is a combination of strengths in each whilst being cheap making it an effective material for prototypes.

Table 2 Hardness indentation statistics

Indentation No.	Length of First Diagonal (μm)	Length of First Diagonal (μm)	HV (kgf/mm^2)	H(MPa)
1	162.99	166.65	68.3	669.8
2	158.95	154.73	69.4	680.6
3	168.69	161.88	67.9	665.9
4	161.49	162.84	70.5	691.4
5	163.97	162.3	69.7	683.5

Average: 69.16 with standard deviation of 0.946

Table 2 shows how the values associated with the indentation photographs taken. This table links with Tabor's construction on figure 7. The values of Vickers hardness we calculated conclusively shows us how Tabor's construction works and is an accurate way of determining hardness of a material.

4.3. Equations

Equations should be centred and numbered in the right end of the line. For further details about equations, symbols, and units, see IC Aero Report Style Guide.

$$R = \frac{\rho L}{A} \quad (1)$$

$$S\epsilon = \frac{\Delta R}{R} \quad (2)$$

$$Vg = Vin \frac{\Delta R_1}{4R} \quad (3)$$

$$\epsilon_n = \frac{4Vg}{VinS} \quad (4)$$

$$V = Vg GAIN \quad (5)$$

$$\epsilon_n = \frac{4V}{VinS GAIN} \quad (6)$$

$$H = \frac{F}{A} \quad (7)$$

$$HV = \frac{2\sin(68)}{d^2} F \quad (8)$$

5. Conclusions

At the end of the experiment, we were able to deduce that metallic alloys such as aluminium have great ductility and strength as well as being very light making it an effective material for aerospace applications. Along with this we were able to use Tabor's construction and evaluate its efficacy with real materials and showed how it is a consistent way to get an accurate value for the hardness of a material. Another aim we successfully concluded was the accuracy of the true and nominal strain curves which match up with historic evidence as to how they should look, and they correlate allowing us to identify what is happening on the molecular scale. The experiments conducted took place in good time and sufficient values could be taken but with more time we could have reduced anomalies in our readings further to increase the accuracy of our graphs and get closer the real values of Young's Modulus, ductility, ultimate tensile strength and so on. Included in this, our hardness photographs exhibited slight amounts of pile-up and sink in which gives us inaccurate values of hardness so this could have been mitigated by using multiple more tests to eliminate anomalies. Finally, for the Wheatstone bridge the use of the dummy gauge would increase our precision as less thermal strain would be considered in our measurement.

References

- (1) Kelvin L. V. Contact electricity of metals. *The London, Edinburgh, and Dublin Philosophical Magazine and Journal of Science*. 1898; 46 (278): 82-120.
- (2) Behaviour of simple beams Handout 1 Imperial College London page 3
- (3) Behaviour of simple beams Handout 1 Imperial College London page 5
- (4) Behaviour of simple beams Handout 2 Imperial College London page 4
- (5) Tabor D. The hardness and strength of metals. *J. Inst.Metals*. 1951; 79 1.
- (6) Behaviour of simple beams Handout 1 Imperial College London page 8

Appendix

Load	Amplified Vg	Stress	Strain
0	0	0	0
500	0.0039	18.32981624	1.14816E-05
1000	0.0078	36.65963248	2.29631E-05
1500	0.0116	54.98944871	3.41503E-05
2000	0.016	73.31926495	4.71038E-05
2500	0.0202	91.64908119	5.94686E-05
3000	0.0245	109.9788974	7.21278E-05
3500	0.0289	128.3087137	8.50813E-05

Raw data values for the loading of copper in which amplified voltage was measured and stress strain calculated in excel. This was repeated for all the materials (aluminium and brass with loading and unloading) before analysing the data for potential anomalies and plotting the figures.